RSC Advances

ROYAL SOCIETY OF CHEMISTRY

www.rsc.org/advances

Different roles of CNTs in hierarchical HZSM-5 synthesis with hydrothermal and steam-assisted crystallization

Yuan Qiu, Li Wang, Xiangwen Zhang, Guozhu Liu*

Key Laboratory for Green Chemical Technology of Ministry of Education, School of Chemical Engineering and Technology, Tianjin University, Tianjin 300072, P. R. China

*The corresponding author: Tel. /fax: 86-22-27892340, Email: gliu@tju.edu.cn (G. Liu)

Abstract: The hierarchical HZSM-5 zeolites with uniform mesopore distribution were synthesized by hydrothermal synthesis (HTS) and steam-assisted crystallization (SAC) methods using multi-walled carbon nanotubes (CNTs) as hard templates. Compared with HTS way, the SAC method favored the utilization of CNTs because of lower phase separation degree. It was also found that the crystallization process of HZSM-5 was slowed down after the addition of CNTs in HTS method, while was accelerated in SAC method. Furthermore, after the addition of CNTs, the hierarchical samples prepared by HTS method showed lower Si/Al ratios and higher acid amounts while slight changes in the acid properties were observed for those prepared by SAC method. The synthesized hierarchical HZSM-5 zeolites using SAC method exhibits similar catalytic activities but better stabilities in the catalytic cracking of n-decane than the HTS samples as a result of presence of more mesopores.

Introduction

HZSM-5 zeolites have been widely used as solid catalysts in petrochemical and fine chemical industries[1-7]. However, the sole presence of micropores in HZSM-5 zeolites hindered the diffusion of larger reactants and products significantly[2]; at the same time, the formation of coke would easily block the micropores and result in deactivation[8]. Compared with micropores, mesopores could enhance the diffusion of lager reactants and tolerate more coke deposit in the channels. Consequently, introducing mesopores into HZSM-5 zeolites seems to be a promising method to promote its catalytic activity and stability. It has been found that the hierarchical zeolites showed a remarkably high resistance to deactivation in various acid-catalyzed reactions[9-13]. Despite that, the mesostructures can also help to stabilize the metal nanoparticles against particle growth and prolong their catalytic lifetimes [14].

Generally, the generation of a secondary porosity in zeolites is achieved by either post-synthetic treatment or template method.[2, 15-18] The post-synthetic treatment method, such as dealumination and desilication will always destroy the integrity of zeolite structures[2, 15, 16], and it is hard to generate uniform mesopores.[10] The mesopores can also be achieved by the addition of a mesoporous template. Compared with the post-synthetic treatment method, the mesopores achieved by using mesoporous templates exhibited more precise control of the mesopore size.[19] The mesoporous templates could be divided into two categories: soft-templates and hard-templates. Usually soft-templates like surfactant micelles and silylated polymers, need to keep sufficient affinity with zeolite frameworks to avoid the formation of separated phases.[10] Recently, Ryoo and co-workers[11] successfully synthesized MFI zeolite nanosheets using a

diquaternary ammonium surfactant in the absence of a second template. Compared with organic molecules, the hard-temples, like carbon materials, usually have less effect on the zeolite structure because of the weaker interaction with synthesis materials, which is beneficial for the reservation of the high crystallinity of zeolites. Besides, in this method, the resultant mesostructure can be simply tailored by using different carbon materials. Thanks to the high aspect ratio and adjustable diameter, the CNTs as hard-templates, performed excellently in hierarchical zeolite synthesis[20, 21]. The zeolite particles can be synthesized outside or inside the CNTs, getting intra or intercrystal mesopores. Schmidt *et al*.[21] synthesized silicalite-1 with uniform mesopores using CNTs as mesopore-forming agents by impregnation method. Tang *et al*.[22] obtained nanosized ZSM-5 of 30-60 nm by confined space synthesis method using CNTs as inert matrix. Schmidt *et al*.[20] found that the CNT-templated SAPO-34 had higher catalysis efficiency compared with carbon particle-templated ones because of the better accessibility of reactants into the interior micropores. When using carbon materials as hard-templates, the phase separation problem would severely decreased the templates utilization efficiency [23]. Steam-assisted conversion (SAC), as a kind of dry gel conversion (DGC) method, is reported effective in decreasing the phase separation degree.[24] However, the influence of the CNTs hard templates on the crystallization process of both HTS and DGC methods is seldom discussed, which may affect the mesoporous properties, acid properties, and thus the catalytic ability.

In this work, we obtained hierarchical HZSM-5 zeolites by both SAC and HTS methods using CNTs as template. The morphology, mesostructure and acid properties of the synthesized hierarchical zeolites were compared according to different methods. The influence of CNTs on zeolite crystallization was investigated by various technologies, like scanning electron microscope

(SEM), X-ray powder diffraction (XRD) and transmission electron microscopy (TEM). It was found that the CNTs hindered zeolite nucleation and growth in HTS method, but accelerated the crystallization process in SAC method, which led to the differences in acid properties of HZSM-5 zeolite. From the catalytic cracking of n-decane, we found that the hierarchical samples showed better stability because of the presence of mesopores. In addition, the hierarchical HTS sample showed higher initial activity than the conventional one because of better acid property.

2. Experimental Section

2.1 Materials

The materials used in the synthesis include ethyl orthosilicate (TEOS, 98%, Tianjin Kermel Chemical Reagent Co. Ltd, China), aluminum nitrate ($Al(NO_3)_3 \cdot 9H_2O$, > 99%, Guangfu, Tianjin, China), tetra-n-propylammonium hydroxide (TPAOH, 25% in water, J&K China Chemical Ltd. Beijing, China), multi-walled CNTs (MWCNT, OD: 8 - 15 nm, length: ~50 μm, > 95%, Chengdu Organic Chemicals Co., China), concentrated hydrochloric acid (Tianjin Jiangtian Technology Co. Ltd, China) and n-decane (AR, Guangfu, Tianjin, China).

2.2 Synthesis

Before being used, the multi-walled CNTs were heated at 100 °C with concentrated hydrochloric acid by a solid-liquid ratio of 2 mg/100 mL for 6 hours to remove the metallic impurity.

In a typical synthesis, aluminum nitrate was dissolved in distilled water before the TPAOH

aqueous solution was added. Then, TEOS was added dropwise to the above solution. The molar composition of the mixture was Al: Si: TPAOH: H_2O = 1: 60: 15.6: 5400. The obtained mixture was denoted as M_0.

In the synthesis of conventional zeolites, M_0 was stirred for 24 h to obtain a clear solution and used for ZSM-5 synthesis. While, for CNT-templated zeolites synthesis, the calculated amount of CNTs ranging from 0 to 30 wt% (mass ratio of CNTs to TEOS) were added to M_0 after it was stirred for 12 h. Finally, the solution was subjected to ultrasound (40 KHz) for 0.5 h followed by another stirring of 12 h.

In the case of HTS method, the obtained mixtures above were transferred to Teflon-coated autoclave and heated at 175 °C for 1 - 24 h by quenching the autoclaves with cold water. The solid products were collected by centrifugation, washed by distilled water and dried at 110 °C overnight. In the case of SAC method, the mixtures were dried at 80 °C overnight and then grinded into fine powder. These powders were then put in a bowl made of PTEE and transferred to Teflon-coated autoclave with water below (4 mL for 100 mL autoclave). The autoclaves were heated at 175 °C for 1 - 24 h by quenching the autoclave with cold water. The solid product was collected and dried at 110°C overnight. The obtained samples with different amounts of CNTs addition were labeled as HTS-x or SAC-x. "x" denotes the percentage of mass ratio of CNTs to TEOS (0 - 30)."

Before used for catalytic cracking reaction and characterization, the samples were calcined in air at 600 °C for 10 h to remove the CNTs and organic templates.

2.3 Characterization

The X-Ray powder diffraction (XRD) patterns were recorded with a Rigaku instrument (D-max 2500, Cu Kα radiation) in the range of 5 - 55° at the rate of 8 °/min. The specific surface area of zeolites was determined by Brunauer-Emmett-Teller (BET) method from N_2 adsorption data at -196 °C on a Tristar 3000 instrument. The total pore volume corresponds to the nitrogen volume adsorbed at P/P_0 = 0.99. The micropore surface areas and micropore volumes were determined from the t-plot method.[25] The pore-size distribution was calculated using the Barret-Joyner-Halenda (BJH) model.[26] Scanning electron microscopy (SEM) images were obtained by FEI Nanosem 430 at accelerating voltage of 0.1 - 30 KV. The amount of Si or Al was quantified by inductively coupled plasma-atomic emission spectrometer (ICP-AES, PROFILE SPEC, Leeman Labs, USA) after dissolving the samples in HF solution. Solid state ^{27}Al spectra were recorded on Infinityplus 300 instrument of 7.0 T (300 MHz) magnetic fields with a 4 mm MAS probe head. Emission transmission (TEM) images were obtained by a JEOL JEM-2100F field emission transmission electron microscope operating at 200 kV.

Ammonia-temperature programmed desorption (NH_3-TPD) was conducted on a Micromeritics 2910 (TPD/TPR) instrument. Previously, the 0.05 g samples were outgassed under an Ar flow at 300 °C for 1 h. After cooling to 50 °C, sequences of ammonia of 1 mL were injected into the system until the samples were saturated. Then, the physical-adsorbed ammonia was removed by flowing He at 100 °C for 60 min. Finally, the desorption experiment of ammonia was carried out in the range of 100-600 °C at a heating rate of 10 °C/min under a He flow (30 cc/min). The desorbed ammonia was detected by thermal conductivity detector (TCD) simultaneously.

The catalytic cracking of n-decane was carried out in a fixed-bed reactor at 500 °C under 15 ccm/min of N_2 stream. A typical procedure is as follows: 0.25 g zeolite (20 - 40 mesh) diluted by

1g silica sand was fixed in the middle of the reactor (OD: 1 cm). After activation in flowing N_2 at 500 °C for 1 h, the n-decane was feed at a rate of 0.10 ml/min. The product was kept at 250 °C before flowing into the in-situ gas chromatograph (Broker GC 456). A six-way gas valve sample loop system equipped on the chromatographic was used to control the injection of samples. The gas chromatograph was equipped with a PLOT/S capillary column (30 m) for C_1 - C_4 analysis and a PONA capillary column (50 m) for C_{5+} analysis. The switching between the two columns was carried out by a six-way valve on specific residence times. The pressure of the two columns was set as 30 psi and 10 psi, respectively. Measurement conditions were as follows: column initial temperature 40 °C, heating rate 10 °C/min, final temperature 250 °C. The injected samples first flow into PLOT/S capillary column, and then switched into PONA capillary column at 3.6 - 4.85 min.

The coke deposited on the ZSM-5 catalysts after reaction was quantitatively determined by thermogravimetric analysis (TGA Q50) at the temperature range of 100 - 800 °C.

3. Results and discussion

3.1 Textural Properties of the hierarchical HZSM-5 zeolites

The hierarchical HZSM-5 zeolites were synthesized with different amount of CNTs by both HTS and SAC methods. All the samples exhibit a typical MFI structure indicated from the XRD patterns (Figure 1). Relative crystallinities, calculated according to the peak areas of 22 - 25° (2θ) with HTS-0 as a reference, are listed in Table 1. As it indicated from table 1, in our work, all the samples show similar crystallinity values (ca. 100 ± 15%). Chou *et al.* [23] reported that even that the crystallinity of ZSM-5 decreased first, the carbon-templated zeolite could still get a reasonable

crystallinity by extending the crystallization time. Therefore, the high crystallinities of the samples in our work probably can be attributed to the relative lower CNT amount used and enough crystallization time.

The zeolite particles of HTS-30 and SCA-30 before and after calcination were observed by TEM. As observed from the TEM images in Figure 2, the CNTs are wrapped by zeolite particles for both the HTS and SAC samples before calcination, and the rod-like mesopores appear in the crystals after calcination. From the SEM images in Figure 3, we can see that a lot of CNTs are excluded out of zeolite particles for the HTS samples, while in SAC method the zeolite particles show better homogeneity with CNTs. This may be attributed to the lower phase separation degree between zeolite species and CNTs.[23] The particle size distributions of these samples are given in Figure 4. The average particle size of HTS samples decreases slightly with the addition of CNTs. For SAC samples, many large crystals appear and the particle size shows a broader distribution. Therefore, the zeolite crystallization process of the samples may be influenced by the addition of CNTs, which will be discussed later.

All the nitrogen adsorption–desorption isotherms given in Figure 5 (a, c) exhibit hysteresis loops and the area of the hysteresis curve increases as the amount of CNTs, indicating that the new mesopores are introduced by CNTs after calcination. Besides, the trace mesopores in parent samples can be attributed to the aggregation of ZSM-5 crystals. As for the pore size distributions, the HTS samples show a narrow peak around 16 nm (Figure 5 (b)), which is similar with the outer diameter of CNTs (8 - 15 nm); while, the SAC samples exhibit a lager mesopore diameter of 18 nm (Figure 5 (d)), probably resulting from the aggregation of CNTs. Despite the little difference

between HTS and SAC methods, the mesopore size of zeolite can be tailored by the diameters of CNTs, which is more simple and effective than other ways.

Physicochemical properties of all the HZSM-5 samples are summarized in Table 1. Though comparison, it is found that due to the smaller crystal size and the presence of some fissures, the SAC-0 shows higher mesopore volume and external surface area than HTS-0. The mesopore volume of HZSM-5 increases with the addition of CNTs for both the two synthesis methods; while, the SAC-x samples show a higher improvement in mesopore volume by the addition of CNTs than HTS-x samples, for example, compared with the corresponding SAC-0/HTS-0 samples, the mesopore volume for SAC-10 samples increased by 72% which was so much higher than that (6%) for HTS-10 sample. According to the literature, the higher mesopore volume improvement with CNTs achieved by SAC method can be explained as the lower phase separation degree between synthesis solution and CNTs when it was steam-assisted.[23] Through the SAC method, the mesopore volume reached the highest value of 0.23 cm^3/g with 20 wt% CNT-addition; however, after the peak, it would decrease with the further addition of CNTs, which was probably caused by the seriously intertwining and lower accessibility of CNTs.

3.2 Acid properties of hierarchical HZSM-5 catalysts

The acid properties of HZSM-5 were investigated by NH_3-TPD technology. As shown in Figure 6, two peaks of desorbed ammonia appear, centered at ~180 °C and ~380 °C, corresponding to weak and strong acid site, respectively. The amounts of weak, strong and total acid sites are calculated and listed in Table 2. For HTS sample, the number of acid sites of the samples increases sharply at first with the addition of CNTs, while the increase rate slows down

with further addition. For example, the acid amount of HTS-0 is 0.30 mmol/g, and it increases by 53% after 10 wt% CNT-addition, but only by 8.7 % with further 10 wt% CNT-addition. The SAC samples show a much smaller increase rate with the addition of CNTs than that of HTS samples. The total acid amount of HTS-30 is 93% higher than that of HTS-0, while that amount of SAC-30 is only 7.8 % higher than that of SAC-0. In addition, the peak at ~380 °C of HTS samples migrates slightly to a higher temperature, indicating that the introduction of CNTs also enhances the acid strength, while no shift can be observed for SAC samples.

To explain the acid properties difference between the samples prepared by HTS and SAC methods, different Si/Al ratio ($r_{Si/Al}$) zeolites was tested and the results are shown in Table 2. All samples prepared by HTS method exhibited a higher $r_{Si/Al}$ than the feed value, indicating that compared with silica species, the aluminum species is more difficult to incorporate into the zeolite frameworks in the crystallization condition when TPA^+ ions are selected as structure-directing agents, this is probably because of the polymerization effect of TPA^+ ions on silica species.[27] While, the introduction of CNTs could help aluminum species incorporate into the zeolite framework and the $r_{Si/Al}$ of the HTS samples decreases from 88 to 61 with the introduction of CNTs, which is consistent with the increase of acid amount. The change of the Si/Al ratio will always be one important factor to influence the density of acid sites and thus the acid strength of ZSM-5, as is concluded by NH_3-TPD tests.

3.3 The crystallization process of HZSM-5 with or without CNTs addition

The relative crystallinities of the samples with and without CNTs addition are given in Figure 7. As can be seen, HTS-0 reaches complete crystallization at 2 h, 1 h faster than HTS-10. However,

the SAC samples show a contrary tendency that the SAC-0 shows a slower crystallization rate than SAC-10. The SEM images of the samples at different crystallization times are given in Figure 8 and 9. For HTS crystallization process, the HZSM-5 crystallizes from homogeneous solution and the collected particles show a typical coffin-shaped morphology. For HTS-10, after 2 h and 4 h crystallization, CNTs wrapped by amorphous phase as well as zeolite particles are observed in Figure 8. In addition, HTS-10 obtains lower solid yield than HTS-0 before 6 h crystallization, which is shown in Table 3. Therefore, it is concluded that the addition of CNTs hinders the crystallization process of HZSM-5 under hydrothermal condition. In the SAC method, the zeolite nucleates and grows from dried aluminum silicate gel. As is shown in Figure 9, the dry gel dissolves and some irregular particles appear on the CNTs surface after 2 h crystallization. Then, lots of spherical particles appear at 3 h and reach a full crystallinity. While, for SAC-10, the dissolution of dry gel is accelerated and the spherical particles appear at 2 h, indicating that the addition of CNTs promotes the crystallization of HZSM-5.

TEM images of HTS-10 at 1.5 h are given in Figure 10, exhibiting that a lot of nano-sized particles aggregate along the CNTs. It has been proposed that the aggregation process and the subsequent densification of the small particles would result in the formation of zeolite crystals[28]. Therefore, the addition of CNTs may accelerate the nucleation of zeolite by promoting the aggregation of aluminosilicate species. Brar *et al.* [29] also found that the addition of some substrates would decrease the free energy to zeolite A nucleation. On the other hand, the aggregation of small particles on CNTs can decrease the supersaturation of the solution, which will hinder the nucleation and growth of HZSM-5 in solutions. Besides, the nucleation and growth rate in solutions (homogeneous nucleation) is much higher than that on CNTs surface

(heterogeneous nucleation) because of a much bigger surface area for HTS method[29]. Thus their total crystallization rate drops after the addition of CNTs, and the synthesized samples show a smaller crystal size. When the zeolite is synthesized by SAC method, the zeolite crystals grow by reorganization of the hydrogel through solid-solid transformations. The addition of CNTs will promote the reorganization process by decreasing the energy barrier and thus accelerates the growth rate of HZSM-5. Besides, the addition of CNTs causes the non-uniform nucleation and growth of synthesis materials, so the particle size of the synthesized HZSM-5 shows a boarder distribution.

The Si/Al ratios in solid and liquid product of the HTS samples with different crystallization time are given in Table 3. It is found that Si/Al ratio of HTS-10 in solid ($S_{Si/Al}$) is 54, much lower than that of HTS-0 after 2 h crystallization. This is probably affected by the changes of supersaturation degree of synthesis solution because that the aluminum coordination and the odd Si substitution is largely affected by hydrolysis water amount in sol-gel process.[30] The $S_{Si/Al}$ increases to 56 at 6 h with the abundant formation of zeolite crystals, and the crystallinity of zeolites grows to 91%. After 8 h crystallization, both the crystallinity and $S_{Si/Al}$ almost hold the same. As a result, the as synthesized HTS-10 has a lower Si/Al ratio and thus higher acid amount than HTS-0.

The Al status in HTS-10 and SAC-10, as well as the corresponding parent samples were detected by ^{27}Al MAS NMR test to interpret the incorporation of aluminum species (Figure 11). The ^{27}Al MAS NMR spectra show a sharp peak at 54.4 ppm and an additional peak at 0 ppm, which means that aluminum is located in both tetrahedral and octahedral environments in

HZSM-5 zeolite frameworks.[31] Compared with HTS-0 sample, the peak area of HTS-10 sample at 0 ppm increases obviously, representing that the octahedral (non-framework) aluminum increases with the addition of CNTs in the hydrothermal synthesis. However, the peak area at 0 ppm has no obvious difference between SAC-0 and SAC-10 samples, indicating that the much fewer defects are formed in zeolites through SAC method than HTS method.

3.4 Catalytic cracking of n-decane over conventional and CNT-template HZSM-5 zeolites

Thanks to the relative better mesopore properties, HTS-30 and SAC-20, as well as the corresponding parent samples, are selected to investigate the catalytic activity of the hierarchical HZSM-5. Compared with the corresponding parent samples, both the hierarchical zeolites prepared by HTS and SAC methods exhibit better stability (in Figure 12). After 11.4 h reaction, HTS-0 shows a conversion of 0.35, while HTS-03 still possesses a high conversion of 0.8; the conversion over SAC-20 is 0.94, but that over SAC-0 drops to 0.90. The coke amounts of HTS-0, HTS-30, SAC-0, SAC-20 after reaction are 29.2, 35.2, 31.3, 32.5 mg, respectively. The higher coke amounts formed on hierarchical zeolites can be attributed to higher conversion of n-decane along with TOS. For the conventional samples, most of the carbon is deposited on the surface of zeolite particles, which blocks the micropores of zeolites and decreases their catalytic activity.[32] The introduction of mesopores retards the deactivation of zeolites by pore blockage and thus improves their catalytic stability.

The parent HZSM-5 synthesized by HTS or SAC method shows a similar initial conversion about 0.97, but the SAC samples show a better stability than HTS samples. This can be attributed to the smaller crystal size, the presence of inter-aggregated pores and thus the better diffusion

properties in the SAC samples[3]. However, because of the high stability of the conventional sample synthesized by SAC method, the introduction of mesopores show a much smaller increase in the zeolite stability compared with the HTS samples. Therefore, the introduction of mesopores will exert higher influence on the larger sized zeolite particles which seriously suffers from low diffusion rate and fast deactivation problems. In addition, the increased acid amount caused by the addition of CNTs results in a higher initial conversion of 0.99 over HTS-30. The better performance of the hierarchical zeolites in both catalytic activity and stability can be attributed to the introduction of mesopores as well as the largely protected microporous structures.

4. Conclusions

Hierarchical HZSM-5 with a feed Si/Al ratio of 60 was synthesized with the addition of a series amount of CNTs by HTS and SAC methods. The crystallization process of HTS/SAC-0 and HTS/SAC-10 was investigated and the results demonstrated that the addition of CNTs hindered the crystallization process of HZSM-5 when synthesized by HTS method, but accelerated this process when synthesized by SAC method, which could be attributed to different synthesis mechanisms. Furthermore, the CNTs influenced the Al substitution in the formation of HZSM-5 crystals in HTS method and the acid amounts of zeolite increased with the addition of CNTs, but no obvious changes in acid amounts were observed for SAC samples. The synthesized hierarchical samples were applied to the cracking of n-decane to evaluate their catalytic properties. It was found that both the activity and stability were promoted with the introduction of mesopores resulting from CNTs.

Acknowledgement

The authors gratefully acknowledge financial support from the National Natural Science Foundation of China (Grants 91116001). We also thank Xu Hou and Yawei Shi for assistance with language polishing.

Reference

1. M. Hartmann, *Angew. Chem. Int. Ed. Engl.*, 2004, **43**, 5880-5882.

2. J. Pérez-Ramírez, C. H. Christensen, K. Egeblad, C. H. Christensen and G. C. Groen, *Chem. Soc. Rev.*, 2008, **37**, 2530-2542.

3. H. Konno, T. Tago, Y. Nakasaka, R. Ohnaka, J.-i. Nishimura and T. Masuda, *Microporous Mesoporous Mater.*, 2013, **175**, 25-33.

4. A. Ishihara, K. Inui, T. Hashimoto and H. Nasu, *J. Catal.*, 2012, **295**, 81-90.

5. R. Javaid, K. Urata, S. Furukawa and T. Komatsu, *Appl. Catal. A-Gen.*, 2015, **491**, 100-105.

6. D. Mores, J. Kornatowski, U. Olsbye and B. M. Weckhuysen, *Chem. Eur. J.*, 2011, **17**, 2874-2884.

7. F. L. Bleken, S. Chavan, U. Olsbye, M. Boltz, F. Ocampo and B. Louis, *Appl. Catal. A-Gen.*, 2012, **447–448**, 178–185.

8. K. Urata, S. Furukawa and T. Komatsu, *Appl. Catal. A-Gen.*, 2014, **475**, 335-340.

9. J. Li, X. Li, G. Zhou, W. Wang, C. Wang, S. Komarneni and Y. Wang, *Appl. Catal. A-Gen.*, 2014, **470**, 115-122.

10. Q. Zhang, S. Hu, L. Zhang, Z. Wu, Y. Gong and T. Dou, *Green Chem.*, 2014, **16**, 77-81.

11. M. Choi, K. Na, J. Kim, Y. Sakamoto, O. Terasaki and R. Ryoo, *Nature*, 2009, **461**, 246-249.

12. J. Kim, M. Choi and R. Ryoo, *J. Catal.*, 2010, **269**, 219-228.

13. S. Inagaki, S. Shinoda, Y. Kaneko, K. Takechi, R. Komatsu, Y. Tsuboi, H. Yamazaki, J. N. Kondo and Y. Kubota, *ACS Catal.*, 2012, **3**, 74-78.

14. J.-C. Kim, S. Lee, K. Cho, K. Na, C. Lee and R. Ryoo, *ACS Catal.*, 2014, **4**, 3919-3927.

15. R. Chal, C. Gerardin, M. Bulut and S. Van Donk, *ChemCatChem*, 2011, **3**, 67-81.

16. K. Na, M. Choi and R. Ryoo, *Microporous Mesoporous Mater.*, 2013, **166**, 3-19.

17. J.-B. Koo, N. Jiang, S. Saravanamurugan, M. Bejblová, Z. Musilová, J. Čejka and S.-E. Park, *J. Catal.*, 2010, **276**, 327-334.

18. D. P. Serrano, J. M. Escola and P. Pizarro, *Chem. Soc. Rev.*, 2013, **42**, 4004-4035.

19. D. Serrano and P. Pizarro, *Chem. Soc. Rev.*, 2013, **42**, 4004-4035.

20. F. Schmidt, S. Paasch, E. Brunner and S. Kaskel, *Microporous Mesoporous Mater.*, 2012, **164**, 214-221.

21. I. Schmidt, A. Boisen, E. Gustavsson, K. Ståhl, S. Pehrson, S. Dahl, A. Carlsson and C. J. H. Jacobsen, *Chem. Mater.*, 2001, **13**, 4416-4418.

22. K. Tang and X. Hong, *Adv. Mater. Res.*, 2011, **299**, 1020-1023.

23. C. Chou, C. S. Cundy and A. A. Garforth, in *Nanoporous Materials Iv*, eds. A. Sayari and M. Jaroniec, 2005, vol. 156, pp. 393-400.

24. K. Zhu, J. Sun, H. Zhang, J. Liu and Y. Wang, *J. Nat. Gas Chem.*, 2012, **21**, 215-232.

25. F. Rouquerol, J. Rouquerol and K. Sing, *Adsorption by Powders and Porous Solids Principles, Methodology and Applications. Methods*, Academic Press, San Diego, 1999.

26. E. Barrett, L. Joyner and P. Halenda, *J. Am. Chem. Soc*, 1951, **73**, 373-380.

27. N. H. Ray and R. J. Plaisted, *J. Chem. Soc., Dalton Trans.*, 1983, 475-481.

28. D. P. Serrano and R. van Grieken, *J. Mater. Chem.*, 2001, **11**, 2391-2407.

29. T. Brar, P. France and P. G. Smirniotis, *J. Phys. Chem. B*, 2001, **105**, 5383-5390.

30. M. May, M. Asomoza, T. Lopez and R. Gomez, *Chem. Mater.*, 1997, **9**, 2395-2399.

31. A. Samoson, E. Lippmaa, G. Engelhardt, U. Lohse and H. G. Jerschkewitz, *Chem. Phys. Lett.*, 1987, **134**, 589-592.

32. F. Schmidt, C. Hoffmann, F. Giordanino, S. Bordiga, P. Simon, W. Carrillo-Cabrera and S. Kaskel, *J. Catal.*, 2013, **307**, 238-245.

Table 1. Physical properties of HZSM-5.

Samples	[a]S_{BET} (m^2/g)	[b]S_{extra} (m^2/g)	[c]V_{micro} (cm^3/g)	[d]V_{meso} (cm^3/g)	[e]R (100%)
HTS- 0	359	103	0.12	0.061	100
HTS-10	364	116	0.12	0.065	98
HTS-20	366	122	0.11	0.067	101
HTS-30	374	130	0.11	0.070	104
SAC- 0	383	103	0.13	0.11	101
SAC-10	389	123	0.12	0.19	100
SAC-20	395	132	0.12	0.23	111
SAC-30	384	119	0.12	0.20	110

a: BET surface area; b: External surface area; c: Micropore volume; d: Mesopore volume

d: Relative crystallinity, calcu lated according to the peak areas of 22 - 25° (2θ) with HTS-0 as a reference.

Table 2. Acid properties of HZSM-5.

Samples	Si/Al	Acid sites (mmol NH_3/g)[c]		
		Total	Weak	Strong
HTS- 0	88[a]	0.30	0.09	0.21
HTS-10	64[a]	0.46	0.15	0.31
HTS-20	61[a]	0.50	0.15	0.35
HTS-30	61[a]	0.58	0.17	0.41
SAC- 0	60[b]	0.51	0.11	0.40
SAC-10	60[b]	0.54	0.11	0.43
SAC-20	60[b]	0.55	0.12	0.43
SAC-30	60[b]	0.55	0.12	0.43

a: Tested by ICP method.

b: Equal to the feed ratio of the Si/Al because of the 100% yield.

c: Calculated by TPD results.

Table 3. Changes in Si/Al ratio and solid yield of HZSM-5 at different crystallization times.

Time (h)	HTS- 0			HTS-10		
	Si/Al[b] (solid)	Si/Al[b] (liquid)	Solid yield[a] (%)	Si/Al[b] (solid)	Si/Al[b] (liquid)	Solid yield[a] (%)
2	75	48	74	54	78	66
6	87	43	97	56	74	91
8	87	26	99	62	57	100
24	88	27	100	64	36	100

a: Solid yield at i h = mass of HZSM-5 collected at i h /mass of HZSM-5 collected after 24 crystallization.

b: Tested by ICP.

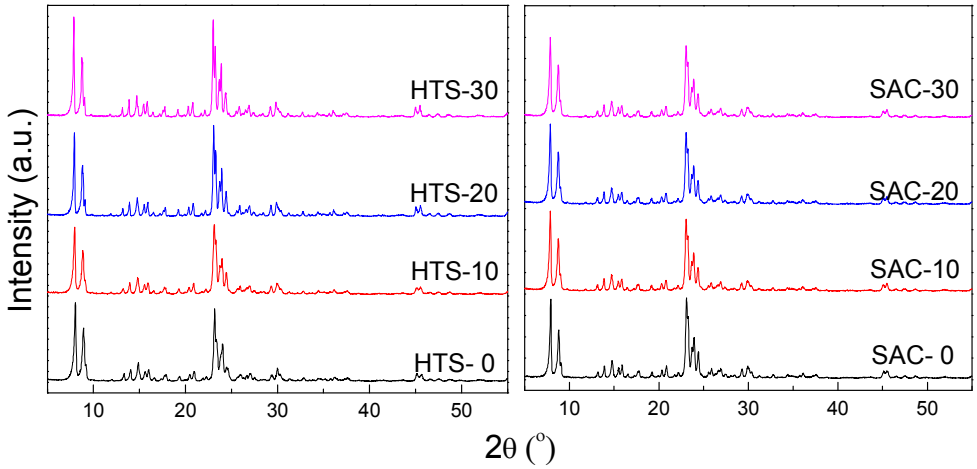

Figure 1. XRD patterns of the conventional and hierarchical HZSM-5 (calcined) synthesized by HTS and SAC methods.

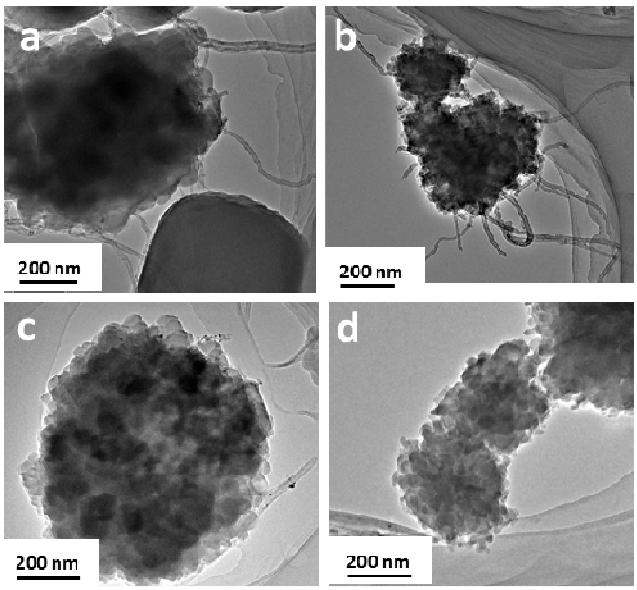

Figure 2. TEM images of hierarchical ZSM-5.
(a, c: HTS-30, before and after calcination; b, d: SAC-30, before and calcination)

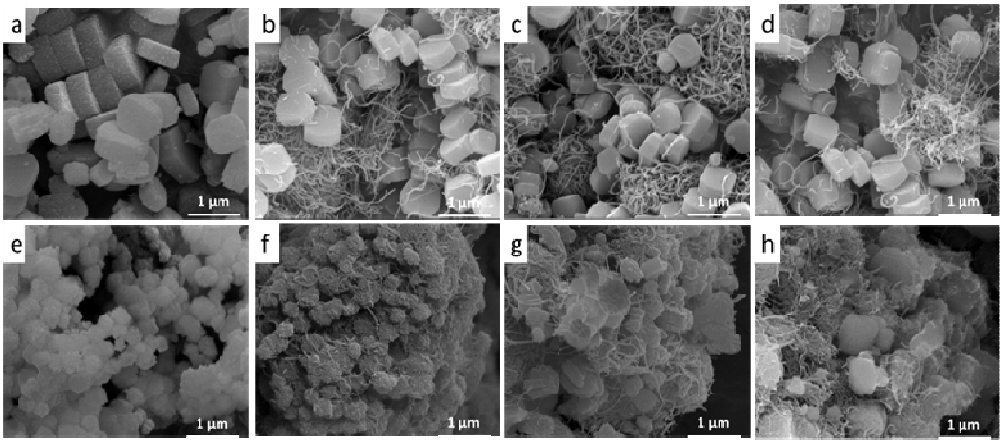

Figure 3. SEM images of conventional and hierarchical HZSM-5 before calcination.
(a, b, c, d: HTS-0, 10 , 20, 30; e, f, g, h: SAC-0, 10, 20, 30)

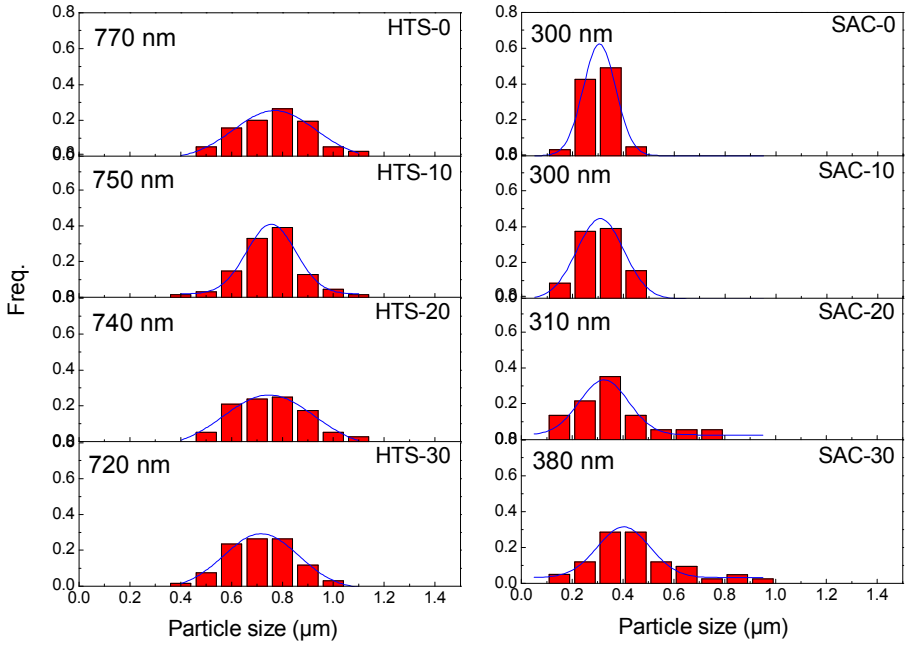

Figure 4. Particle size distribution of HZSM-5.

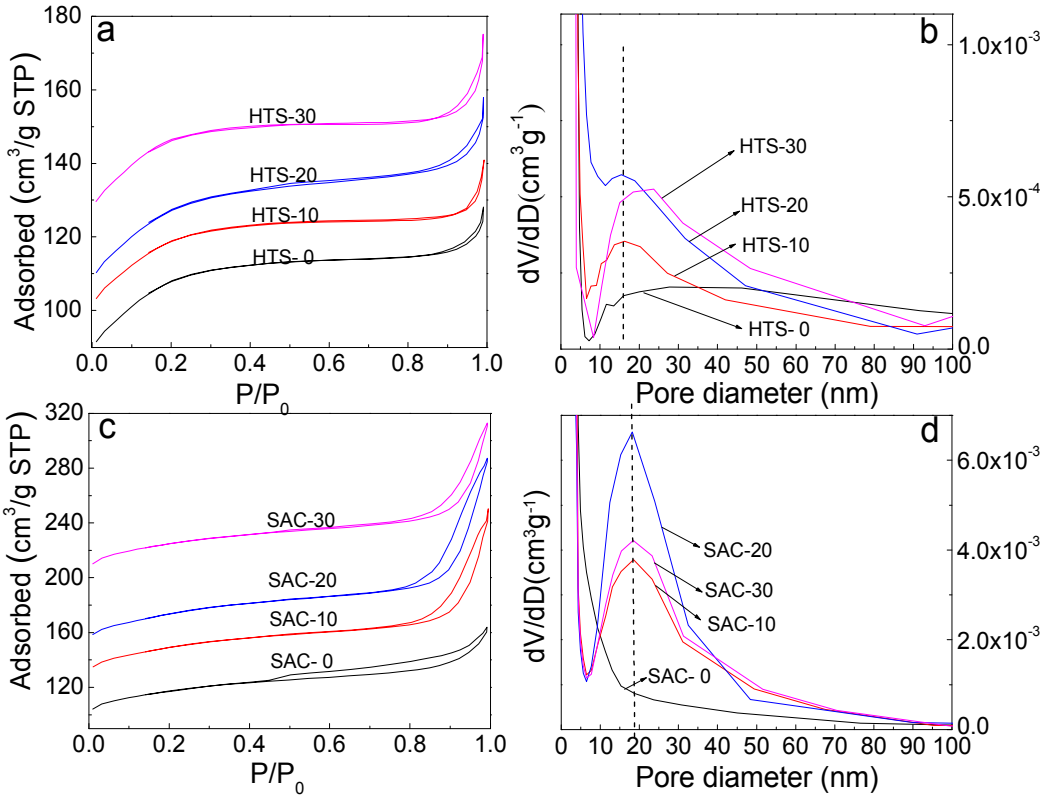

Figure 5. N_2 adsorption-desorption isothermals and pore size distribution of calcined HZSM-5

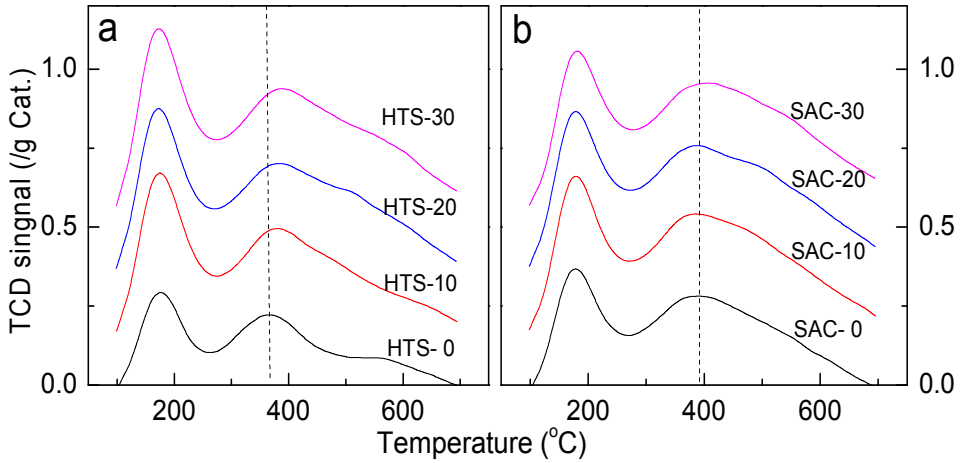

Figure 6. NH_3-TPD curves of conventional and hierarchical HZSM-5.

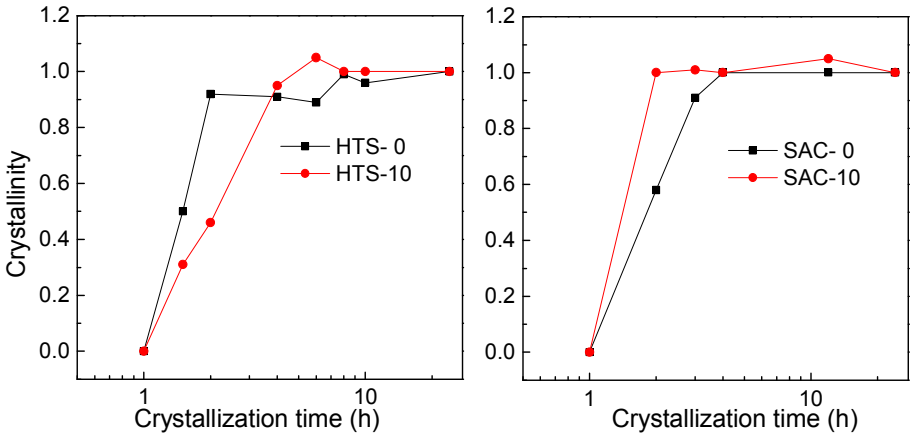

Figure 7. Relative crystallinity of HZSM-5 (calcined) as a function of crystallization time. (Relative crystallinity was determined from the peak area between 2θ = 22 - 25°)

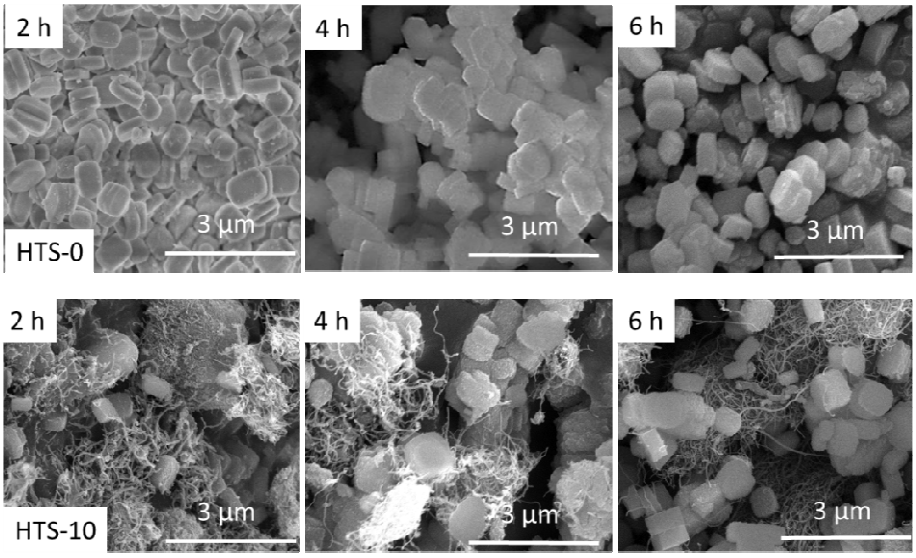

Figure 8. SEM images of HTS-0 and HTS-10 with different crystallization time (not calcined).

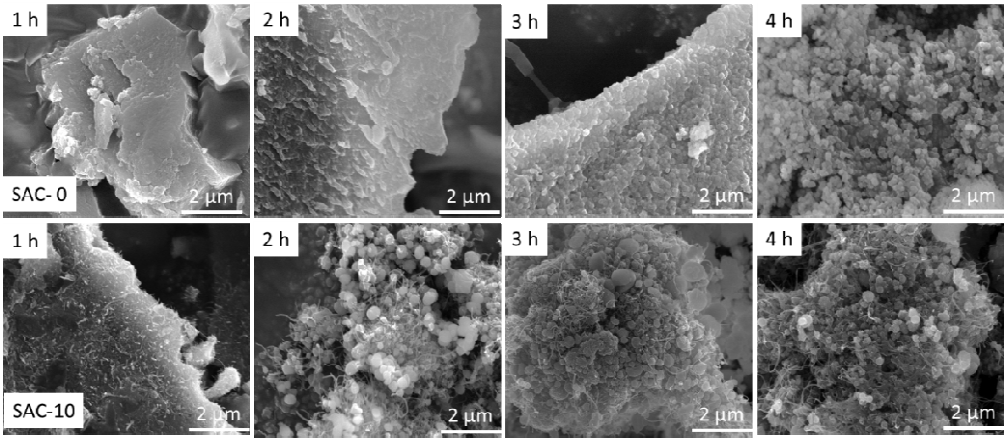

Figure 9. SEM images of SAC-0 and SAC-10 with different crystallization time (not calcined).

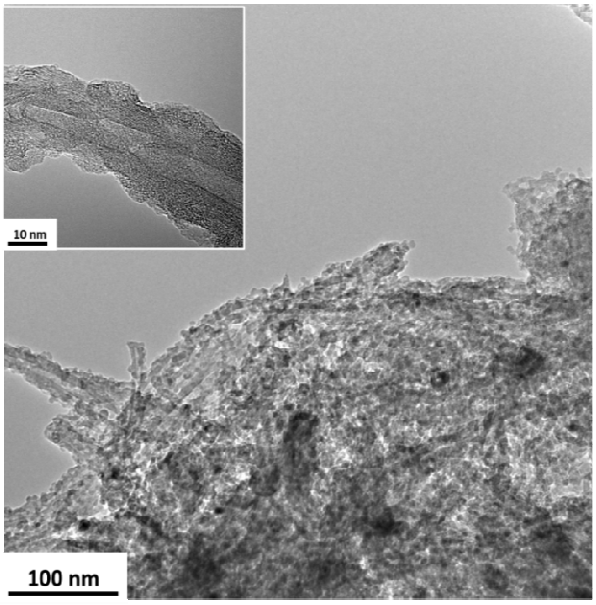

Figure 10. TEM images of the HTS-10 of 1.5 h.

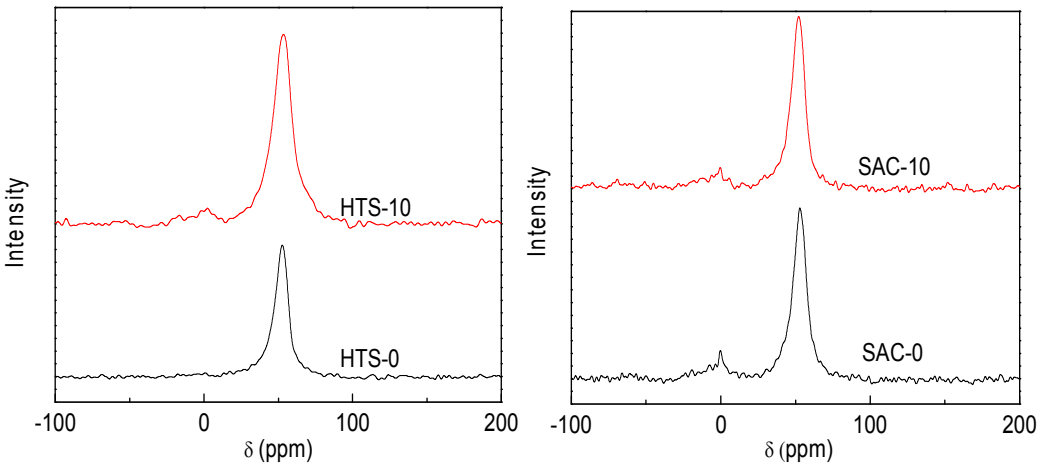

Figure 11. ^{27}Al MAS NMR of HZSM-5 with or without the addition of CNTs.

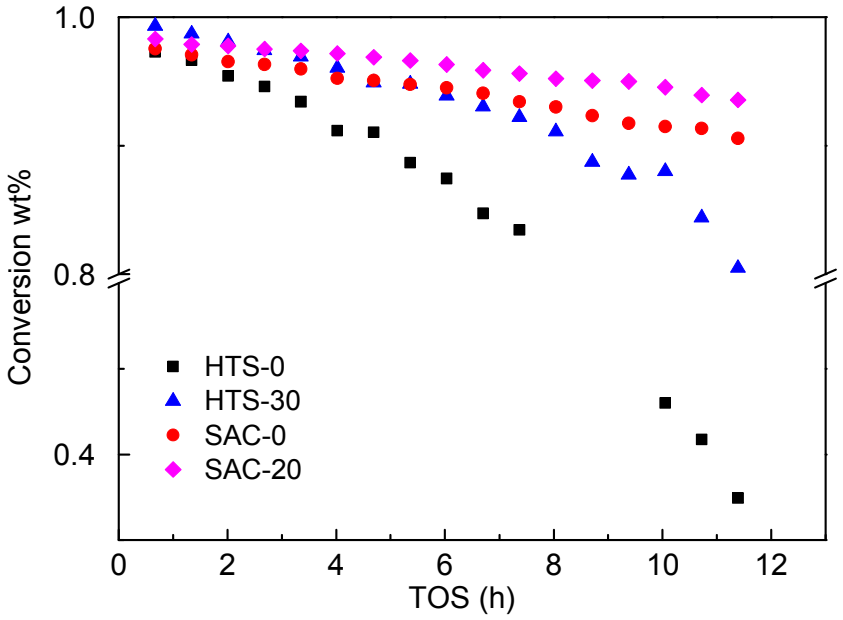

Figure 12. Conversion of n-decane cracking over HZSM-5 as a function of TOS.

For table and contents only